Available online at www.sciencedirect.com
ScienceDirect
International Journal of Pressure Vessels and Piping 85 (2008) 368–377
INTERNATIONAL JOURNAL OF Pressure Vessels and Piping
www.elsevier.com/locate/ijpvp

Oxidation behaviour of an Alloy 617 in very high-temperature air and helium environments

Changheui Jang*, Daejin Lee, Daejong Kim

Department of Nuclear and Quantum Engineering, Korea Advanced Institute of Science and Technology, 373-1 Guseong-dong Yuseong-gu, Daejeon 305-701, Republic of Korea

Abstract

The oxidation characteristics of Alloy 617, a candidate structural material for the key components in the very high-temperature gas-cooled reactor (VHTR), were investigated. High-temperature oxidation tests were conducted at 900 and 1100 °C in air and helium environments and the results were analysed. Alloy 617 showed parabolic oxidation behaviour at 900 °C, but unstable oxidation behaviour at 1100 °C, even in a low oxygen-containing helium environment. The SEM micrographs also revealed that the surface oxides became unstable and non-continuous as the temperature or the exposure time increased. According to the elemental analysis, Cr-rich oxides were formed on the surface and Al-rich discrete internal oxides were formed below the surface oxide layer. After 100 h in 1100 °C air, the Cr-rich surface oxide became unstable and non-continuous, and the matrix elements like Ni and Co were exposed and oxidized. Depletion of grain boundary carbides as well as matrix carbides was observed during the oxidation in both environments. When tensile loading was applied during high-temperature oxidation, the thickness of the surface oxide layer, the internal oxidation, and decarburization were enhanced because of the increase in diffusion of oxidizing agent and gaseous reaction products. Such enhancement would have detrimental effects on the high-temperature mechanical properties, especially the creep resistance of Alloy 617 for the VHTR application.

Keywords: Alloy 617; Oxidation; Creep

1. Introduction

The very high-temperature gas-cooled reactor (VHTR) is currently the most promising reactor type among the generation-IV (Gen-IV) reactors for producing electricity and hydrogen economically. It is a graphite-moderated reactor that uses helium gas to remove the heat generated in the reactor core to the power conversion unit or the hydrogen-production plant. To achieve high thermal efficiency and hydrogen production capability, the helium coolant will be operated at a temperature of about 850 °C or higher [1]. Also, a coolant gas pressure of up to 8 MPa is being considered. Therefore, the structural materials of the VHTR have to survive harsh conditions for the lifetime of the reactor, or up to 60 years. In the VHTR, the high-temperature helium coolant from the reactor core will go through the hot-gas duct and the intermediate heat exchanger where the heat is transferred to the power conversion system and the hydrogen production facility. Among the variety of materials reviewed, several nickel-base superalloys are seriously considered as the materials for these high-temperature components [2].

Nickel-base superalloys, especially the precipitation hardening superalloys, have been widely used in many high-temperature applications because of high-temperature strength, oxidation resistance, creep resistance, and phase stability [2]. However, the proposed operating temperature of the VHTR is so high that the precipitates responsible for the high-temperature strength of those alloys are no longer stable. Because of the dissolution of the precipitates, the precipitation hardening superalloys are not suitable for VHTR application. On the other hand, the solid solution hardening superalloys, that depend on lattice distortion caused by alloying elements for their strength, can maintain considerable strength at higher temperature

*Corresponding author. Tel.: +82 42 869 3824; fax: +82 42 869 3810.
E-mail address: chjang@kaist.ac.kr (C. Jang).

0308-0161/$ - see front matter © 2007 Elsevier Ltd. All rights reserved.
doi:10.1016/j.ijpvp.2007.11.010

[2–4], and are considered suitable for the VHTR application. Among these superalloys are Alloy 617, Haynes 230, and Hastelloy-XR.

When superalloys are exposed to the VHTR coolant for a prolonged period, they will be subjected to degradation due to creep [2,5]. Therefore, the creep properties of the candidate superalloys should be well understood and characterized to be used in design and analysis. In addition, oxidation and other high-temperature corrosion resistance of these superalloys are of concern because they would have effects on the mechanical property degradation of superalloys by metal loss, decarburization, internal oxidation, etc. [5–7]. Therefore, to understand creep resistance of the candidate superalloys, the oxidation behaviour and the stability of oxides should be properly understood. Accordingly, there have been several studies on the high-temperature oxidation of superalloys in various helium environments [7–16]. However, the evolution of oxides and microstructural changes of Alloy 617 during high-temperature oxidation have not been clearly identified. Furthermore, the effects of tensile loading on the oxidation behaviour of Alloy 617 have not been properly investigated.

Therefore, in the present work, the oxidation behaviour of Alloy 617, one of the candidate alloys, were investigated by oxidation tests at 900 and 1100 °C in air and impure helium environments for up to 200 h. The evolution of oxides and microstructural changes during the high-temperature oxidation were also analysed through the scanning electron microscope and elemental analysis of the oxidation tested specimens. Finally, the effects of tensile loading on the oxidation behaviour and microstructural changes were investigated by analysing creep specimens tested in high-temperature air.

2. Experimental procedures

2.1. Test material and specimens

The material used in this study is an 18 mm-thick plate of Inconel Alloy 617. The chemical composition of the material is shown in Table 1. The material was solution annealed at 1175 °C for an hour and water quenched. A typical microstructure is shown in Fig. 1. As shown in the figure, the as-received microstructure contains twins, well-distributed primary carbides and grain boundary carbides. These carbides were known to be primarily $M_{23}C_6$-type carbides precipitated during solution anneal heat treatment in Alloy 617 [8]. According to the supplier's information [12], the average ASTM grain size is 4.6. The mechanical properties at room temperature are summarized in Table 2. As shown in Fig. 2, the oxidation test specimen used in this study is a 1 mm-thick coupon-type specimen. The round bar-type specimen shown in the figure was used in creep tests and analysed to investigate the effects of tensile loading on the oxidation behaviour.

2.2. Test set-up and conditions

The oxidation tests for coupon-type specimens were conducted in air and helium gas environments at 900 and 1100 °C. A box furnace was used for the oxidation tests in air. The specimens were exposed at the test conditions for up to 100 h. In the helium test, the vacuum furnace shown in Fig. 3 was used. The helium gas used in this study is of 99.999% high purity containing small amount of impurities, such as 1.8 ppm H_2O, 1.4 ppm O_2, 3.1 ppm N_2. Before the tests, the vacuum furnace was purged with helium after achieving 10^{-3} Torr vacuum. This process was repeated three times. Then, a constant helium flow rate of 60 cm^3/min was maintained for 5 h at room temperature. Finally, the furnace was heated up to the test temperature in about 2 h. The helium test was conducted up to 200 h

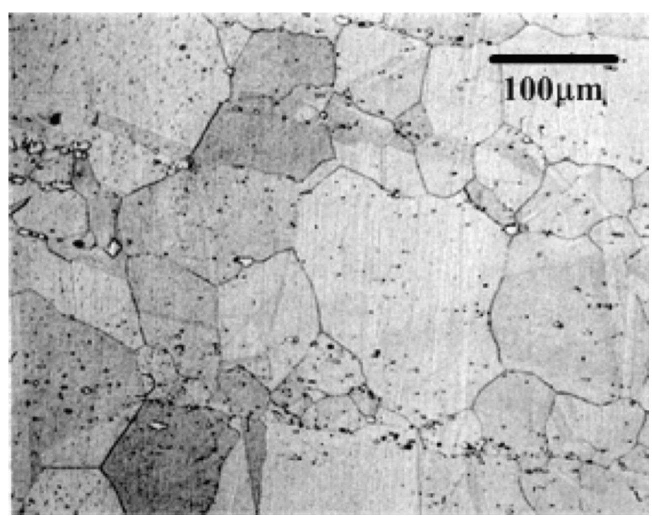

Fig. 1. Microstructure of Alloy 617, as-received condition.

Table 2
Mechanical properties of Alloy 617 at room temperature

Yield strength	Ultimate tensile strength	% Elongation	Reduction of area	Average grain diameter
364 MPa	823 MPa	53.3%	55.9%	71.9 mm

Table 1
Chemical composition of Alloy 617 used in the study

Element	C	Mn	Fe	S	Si	Cu	Ni	Cr	Al	Ti	Co	Mo	P	B
w/o	0.09	0.06	1.16	0.001	0.08	0.05	53.94	21.68	1.14	0.52	11.53	9.74	0.006	0.002